ISTITUTO NAZIONALE DI FISICA NUCLEARE

Sezione di Catania

INFN/TC–11/07
26 October 2011

CALIBRATING THE PHOTOSENSORS FOR THE DCAL EXTENSION OF THE ALICE ELECTROMAGNETIC CALORIMETER: AN ACTIVITY REPORT

F.Astuti, A.Badalà, A.Calivà, A.Grimaldi, V.Indelicato, P. La Rocca, F.Librizzi, G.S.Pappalardo, O.Parasole, C.Petta, F. Riggi

Dipartimento di Fisica e Astronomia, Università di Catania
and INFN, Sezione di Catania

Abstract

The activity carried out to characterize and assemble a final set of about 1700 Avalanche Photo Diodes (APD) to be used in the additional super-modules of the DCAL ALICE electromagnetic calorimeter is described.

PACS.: 06.60.-c , 85.30.-z, 85.60.Dw

Published by ***SIS–Pubblicazioni***
Laboratori Nazionali di Frascati

1 INTRODUCTION

To enhance the performance of the ALICE detector [1], a large acceptance electromagnetic calorimeter has been already built, installed and commissioned. The Electromagnetic Calorimeter of the ALICE experiment consists of 10 EMCal super-modules, subtending the region $\Delta\varphi=180°$ and $|\Delta\eta| < 0.7$, and 6 DCal super-modules subtending 60° in φ and $|\Delta\eta| < 0.7$ (Fig.1). Together, the DCal and EMCal form a two-arm electromagnetic calorimeter, enabling in this way back-to-back correlation measurements. Globally, the EMCal contains 12x24x4x10 = 11520 towers, whereas the DCal contains 12x16x4x6 = 4608 towers, since its super-modules are shorter.

Recently, an extension of the the DCal was approved: it consists of four 1/3 super-modules with the same length as for the EMCal, to be inserted in the orange regions shown in Fig.2. It implies the construction and assembly of additional 1600 towers.

The detailed description of the structure of the electromagnetic calorimeter has been previously reported [2-4], as well as the setup and experimental procedure employed for a full characterization in our laboratory of the Avalanche Photo Diodes for the previous super-modules [5]. This Report describes the activity recently done in Catania to test the Avalanche Photodiodes to be used for these additional 1/3 super-modules and the statistical distributions of the relevant quantities for such devices.

2 DEVICES TO BE TESTED

The APDs chosen for these additional super-modules are of the same type used for the EMCal super-modules (Hamamatsu series S8148 and S8148-1468). During such activity we tested and assembled an additional sample of 1690 APDs. The main characteristics of the sample under test are shown in Figs 3-5. From the breakdown voltage V_{br} and V_{50} distributions we can deduce that almost 99% of APDs would fulfill the condition $V_{30}<400$ V. The values of dark current are spread out over a large range, from few nA up to 20 nA. A clear distinction between the two series of APDs (S8148 and S8148-1468) is evident. A such broad distribution suggested us to check the behaviour of small subsets of APDs, with very different dark currents, as a function of temperature.

3 TEST RESULTS

3.1 Calibration Results

The 1690 APDs were tested and calibrated following the usual procedure used for the former super-modules [5]. The main aim is to find the bias voltage setting to have a gain equal to 30. The distribution of V_{30} evaluated using our procedure is shown in Fig.6. As expected, only 16 APDs over 1690 (i.e. 0.9%) are rejected because V_{30} is over the limit of 400 V.

Our results are in good agreement with those provided by Hamamatsu, since the difference between V_{50} obtained in Catania and the corresponding value reported in Hamamatsu datasheets usually differs by less than 5 V (Fig.7). The systematic shift of the distribution is probably due to the different temperature conditions of the two laboratories (25 °C in Catania and some degrees higher in Japan).

Finally, the voltage coefficient (i.e. the percentage variation in gain for a voltage variation of 1 V) shows a narrow distribution for the whole sample of APDs, as shown in Fig.8, centred at 2.2 %/V.

3.2 Study of the gain dependence on temperature

The dependence of the APD gain on the operational temperature was also investigated for a small sample of devices. Since the temperature coefficient (i.e. the percentage variation in gain for a temperature variation of 1 °C) depends on the dark current, we selected 25 APDs with dark currents ranging over the whole available current range. The selected APDs were tested at different temperatures, from 22 °C to 29 °C. The anticorrelation between gain and temperature is shown in Fig.9 for the 25 APDs under test. The temperature coefficient extracted from these data slightly depends on the APD dark current, as shown in Fig. 10. As a consequence, the distribution in Fig.11 is broader than usual and it is centred at -1.91%/°C.

3.3 APD Classification

According to their V_{30} value, the APDs are classified into different quality ranges, indicated with different colour codes. The following Table lists the colour codes adopted for the DCal super-modules and the number of APDs satisfying those specific V_{30} ranges.

Only ORANGE and RED APDs are rejected. For the sample under study it corresponds to 16 APDs, that means less than 1%.

Table I: List of the colour codes used to classifythe APDs depending on their V_{30} voltage.

COLOUR	V30 lower limit	V30 upper limit	Number of APDs
VIOLET	0	290	0
WHITE	290	315	0
PINK	315	330	7
GOLD	330	345	179
SILVER	345	355	187
BLUE	355	370	419
GREEN	370	390	716
YELLOW	390	400	164
ORANGE	400	410	16
RED	410	450	0

3.4 Work progress

The different phases of the work were monitored due to the strict deadlines. The first step of the work is the soldering of APDs to preamplifier: during this phase, a unique correspondence between the APD SN (provided by Hamamatsu) and the CSP SN (that is an internal code) is made. Once the APDs are soldered and calibrated, they have to be glued to the light guides which allow to couple the photosensors to the WLS optical fibres that transport the scintillation light produced inside the towers of the electromagnetic calorimeters.

In Fig. 12 the progress of the 3 main work phases (soldering, calibration and gluing) is shown as a function of the time: the three works proceeded in the same way and the whole work was completed in less than 2 months.

4 REFERENCES

[1] The ALICE Collaboration, Journal of Instrumentation, 2008_JINST_3_S08002 (2008).
[2] The ALICE Collaboration, The Electromagnetic Calorimeter, Addendum to the Technical Design Report, CERN-LHCC-2006-014.
[3] The ALICE Collaboration, The Electromagnetic Calorimeter, Technical Design Report CERN-LHCC-2008/014.
[4] he ALICE Collaboration, ALICE DCAL: An addendum to the EMCal Technical Design Report, Di-jet and hadron-jet correlation measurements in ALICE, CERN-LHCC-2010-011.
[5] F.Astuti et al., Report INFN/ TC-08/ (2008).

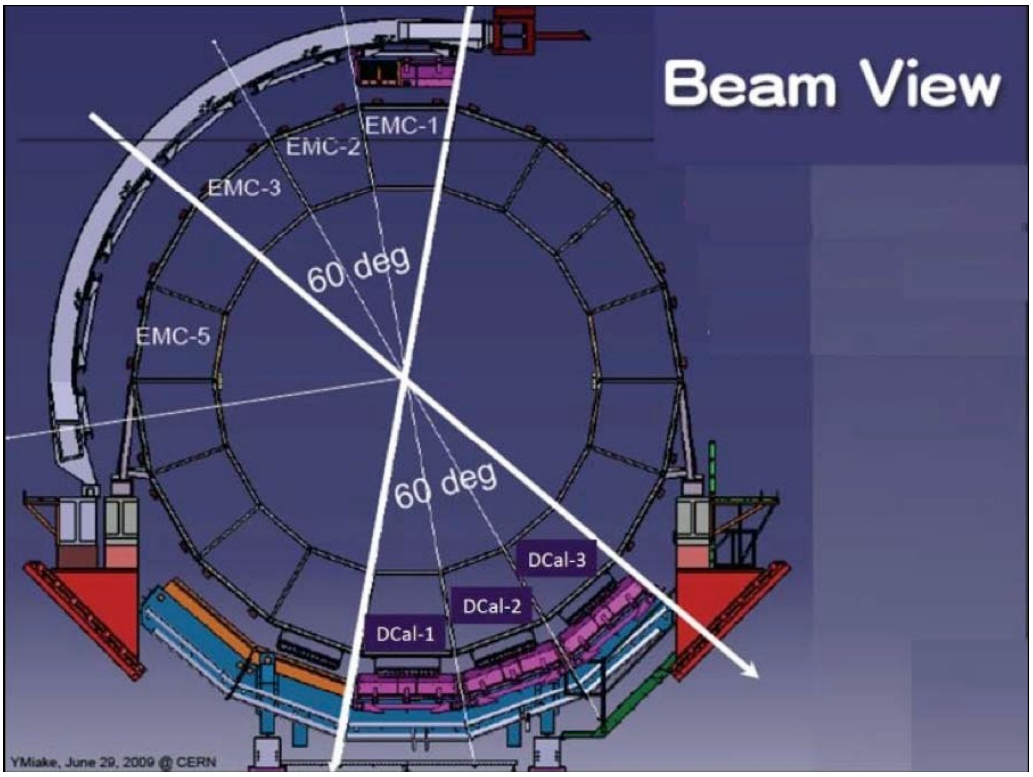

Fig. 1: Layout of the overall structure of the ALICE Electromagnetic Calorimeter.

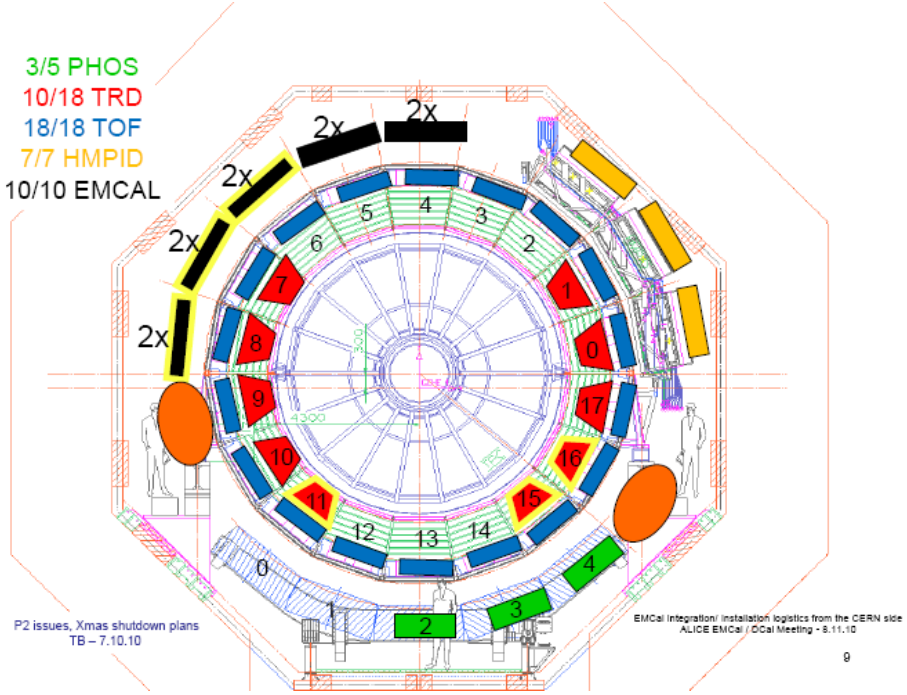

Fig. 2: Last extension of the ALICE Electromagnetic Calorimeter. The additional super-modules will be inserted in the regions indicated in orange.

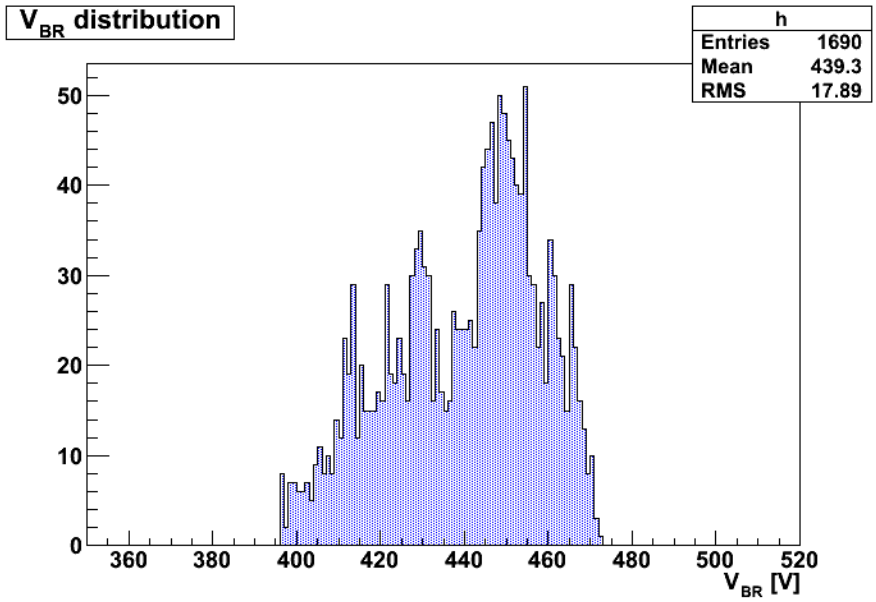

Fig. 3: Breakdown voltage distribution as provided by Hamamatsu.

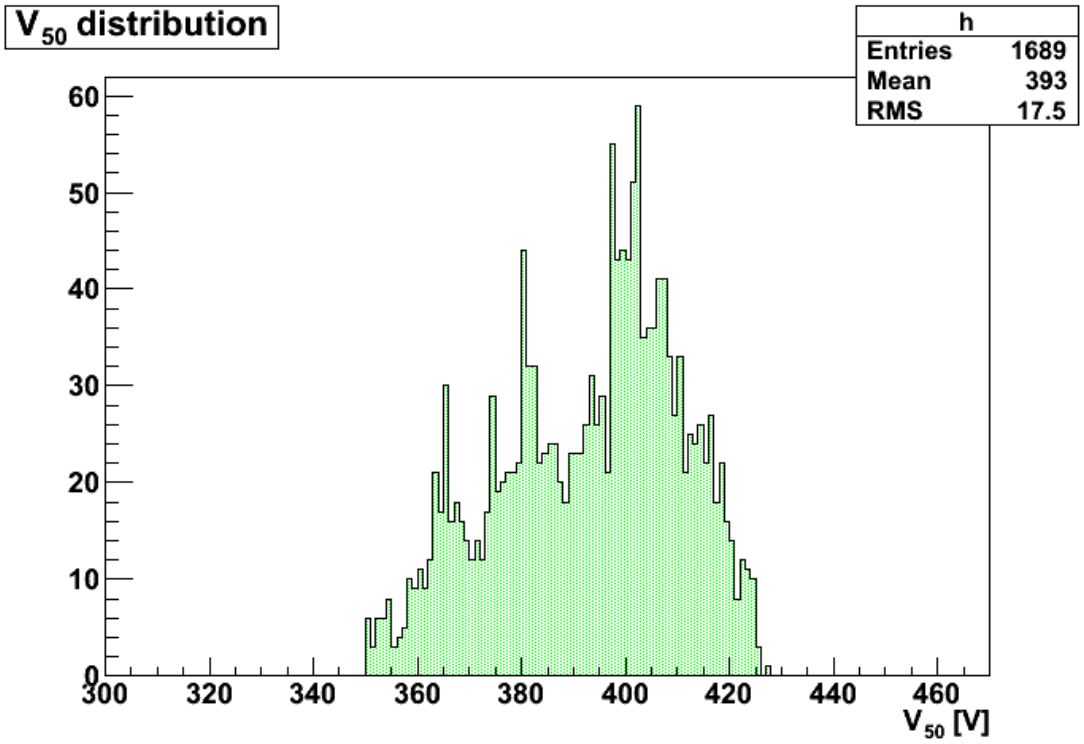

Fig. 4: Voltage V_{50} distribution as provided by Hamamatsu.

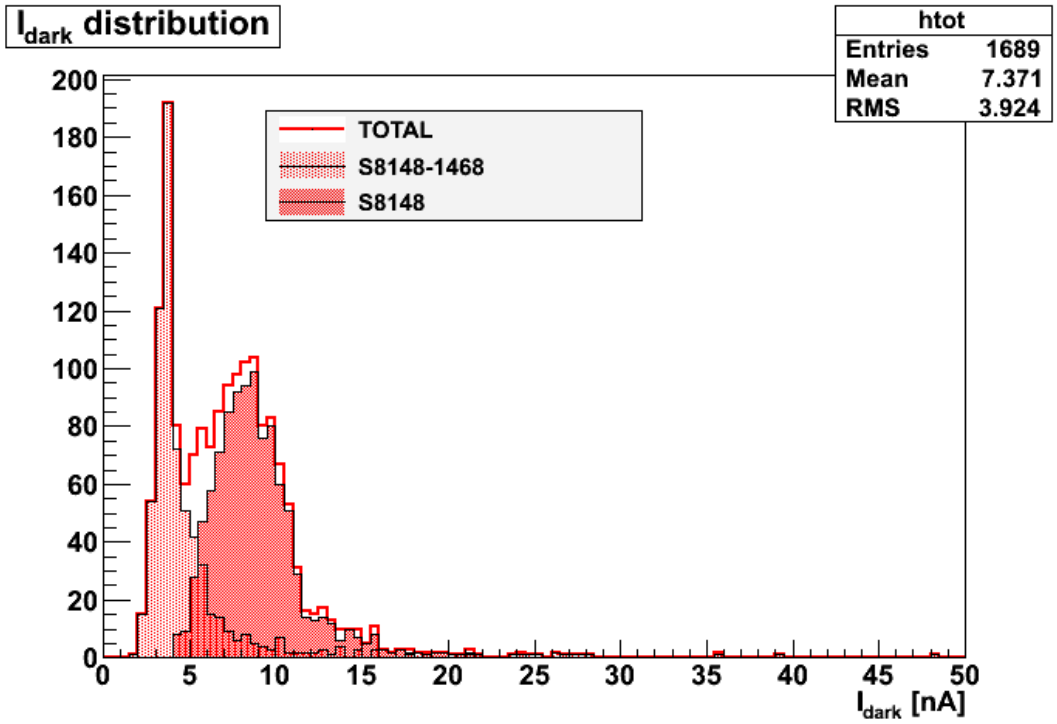

Fig. 5: I_{dark} distribution as provided by Hamamatsu. The 3 histograms refers to the two series of APDs (S8148 and S8148-1468) and to their total.

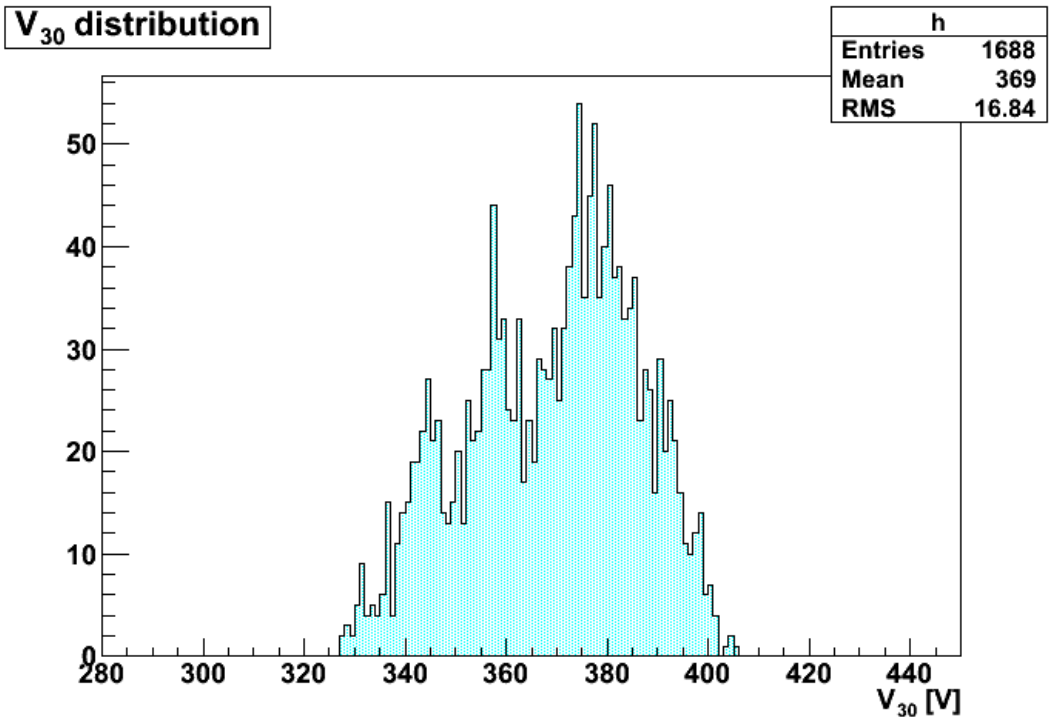

Fig. 6: Voltage V_{30} distribution obtained in Catania laboratory.

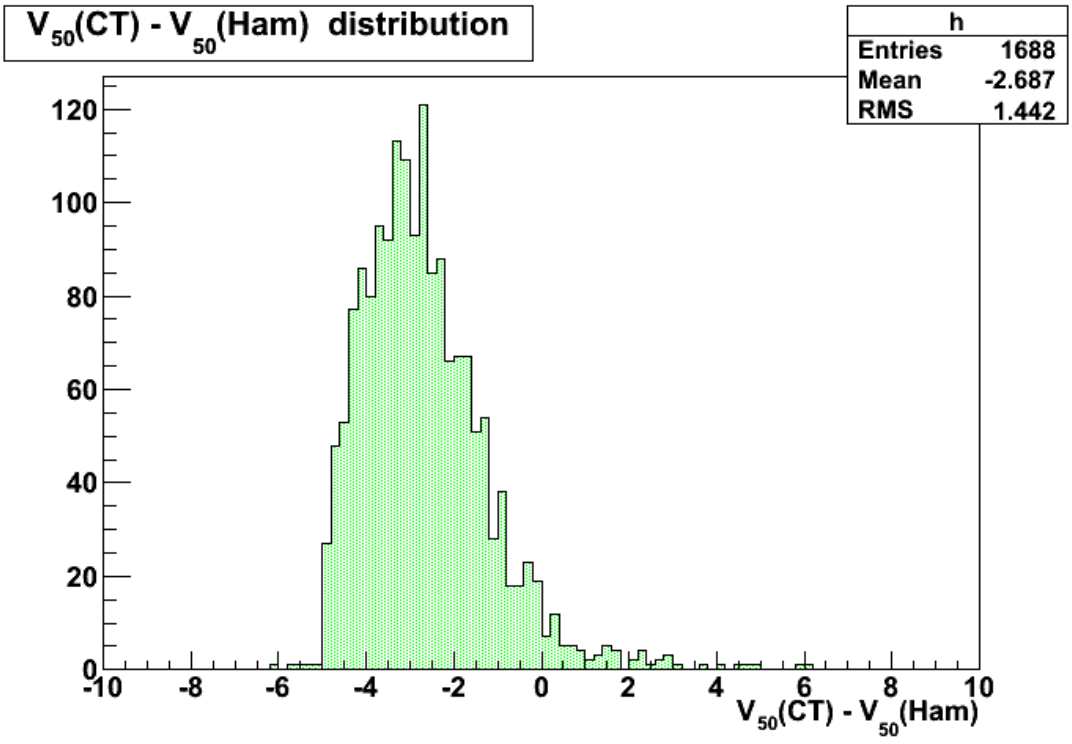

Fig. 7: Difference between the values of V_{50} obtained by our test procedure and by Hamamatsu.

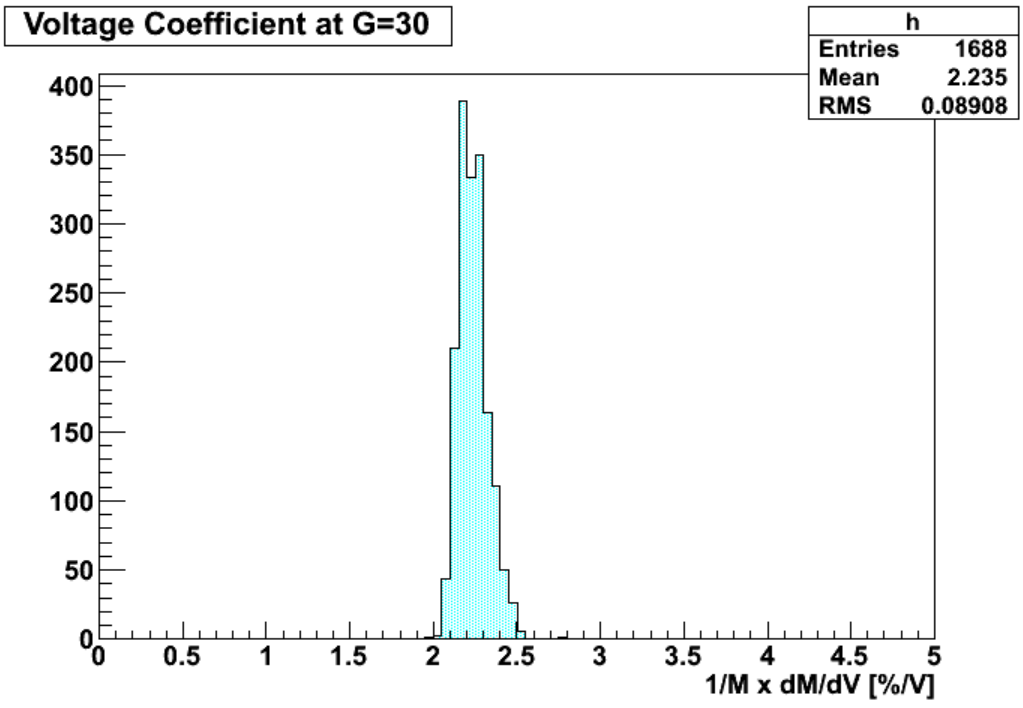

Fig. 8: Voltage Coefficient distribution.

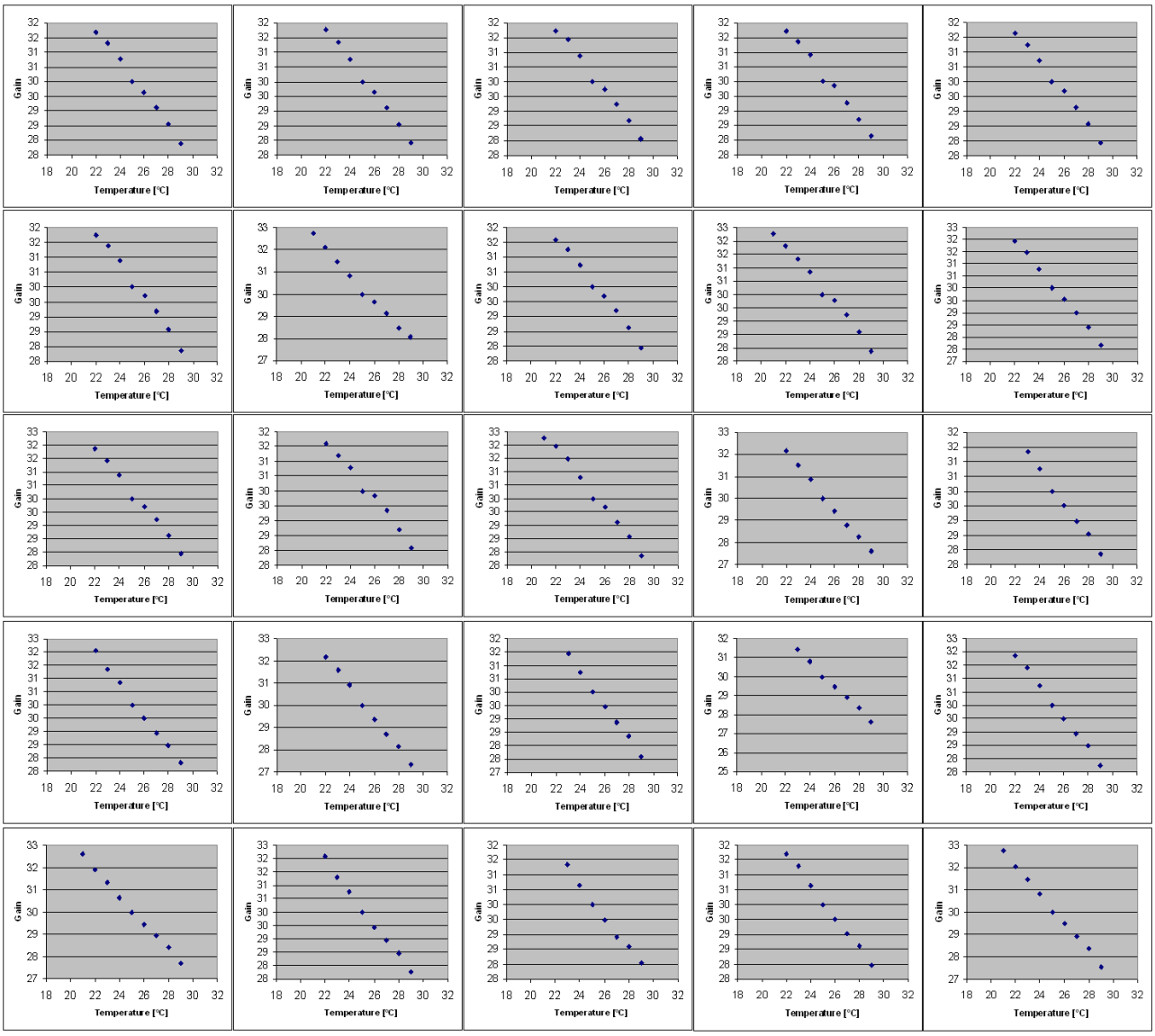

Fig. 9: APD gain as a function of temperature, for the 25 APDs under investigation.

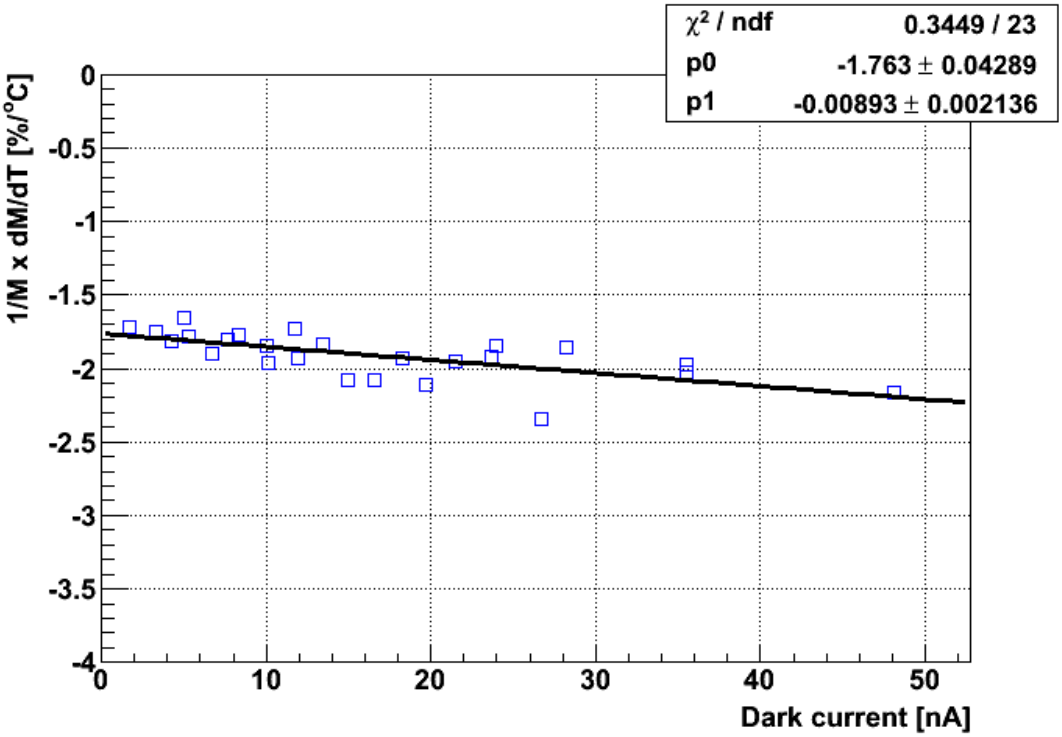

Fig. 10: Temperature coefficient as a function of dark current.

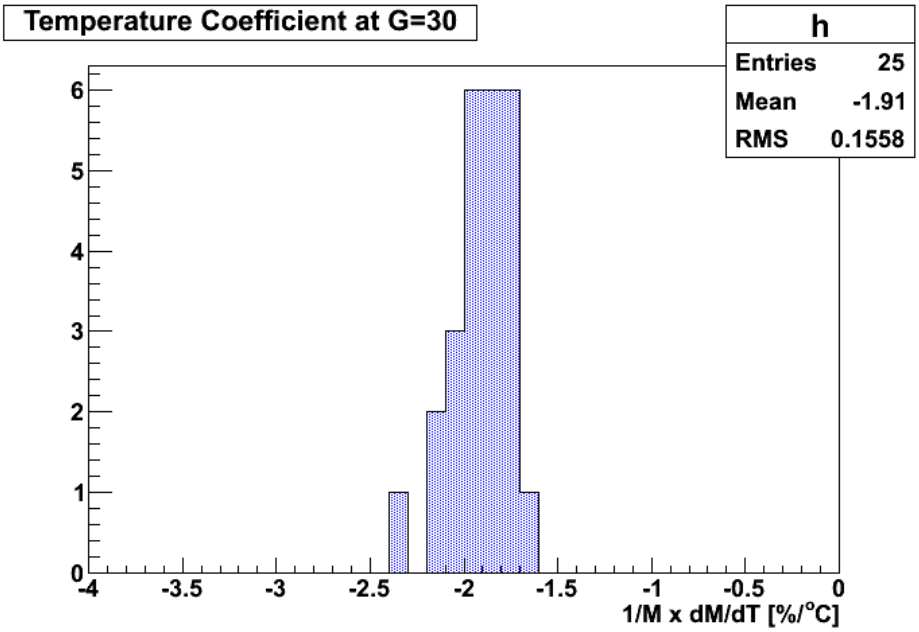

Fig. 11: Temperature coefficient distribution.

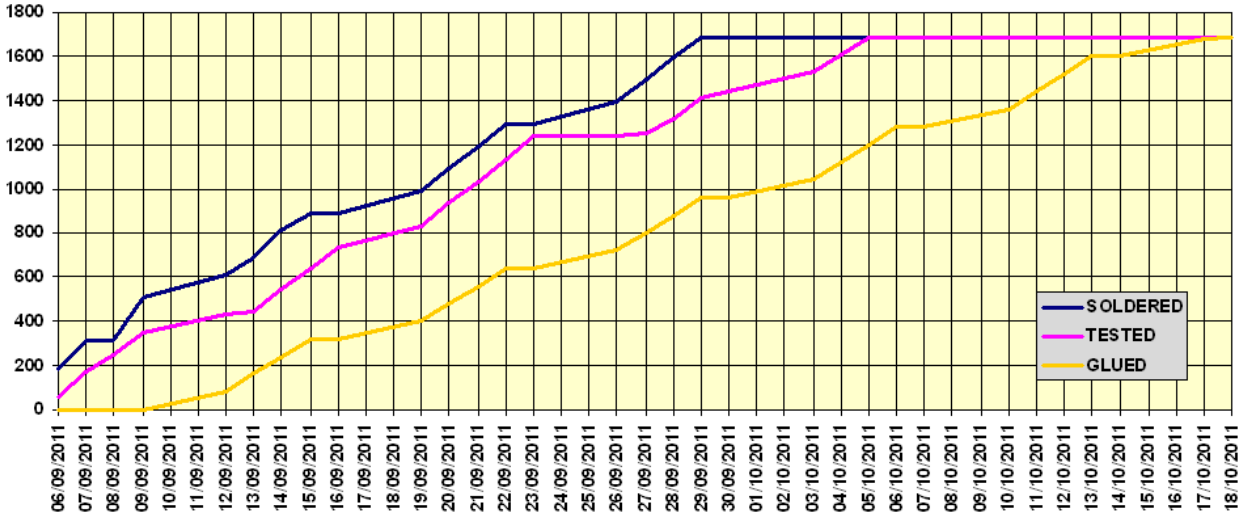

Fig. 12: Time progression of the different working phases.